



Jackson, D. R., Shakya, G., Patel, A. B., Mohammed, L. Y., Vasilakis, K., Wattana-Amorn, P., Valentic, T. R., Milligan, J. C., Crump, M. P., Crosby, J., & Tsai, S. C. (2018). Structural and Functional Studies of the Daunorubicin Priming Ketosynthase DpsC. *ACS Chemical Biology*, 13(1), 141-151. <https://doi.org/10.1021/acschembio.7b00551>

Peer reviewed version

Link to published version (if available):
[10.1021/acschembio.7b00551](https://doi.org/10.1021/acschembio.7b00551)

[Link to publication record in Explore Bristol Research](#)
PDF-document

This is the author accepted manuscript (AAM). The final published version (version of record) is available online via ACS at <https://pubs.acs.org/doi/10.1021/acschembio.7b00551> . Please refer to any applicable terms of use of the publisher.

University of Bristol - Explore Bristol Research

General rights

This document is made available in accordance with publisher policies. Please cite only the published version using the reference above. Full terms of use are available:
<http://www.bristol.ac.uk/red/research-policy/pure/user-guides/ebr-terms/>

Supporting Information

Structural and Functional Studies of the Daunorubicin Priming Ketosynthase

DpsC

David R. Jackson¹, Gaurav Shakya¹, Avinash B. Patel¹, Lina Y. Mohammed², Kostas Vasilakis², Pakorn Wattana-Amorn², Timothy R. Valentic¹, Jacob Milligan¹, Matthew P. Crump², John Crosby², and Shiou-Chuan Tsai¹

1. Departments of Molecular Biology and Biochemistry, Chemistry, and Pharmaceutical Sciences, University of California, Irvine, Irvine, CA 92697.

2. School of Chemistry, University of Bristol, United Kingdom, Bristol BS8 1TS, United Kingdom.

Corresponding authors: Shiou-Chuan Tsai. Department of Molecular Biology and Biochemistry, Department of Chemistry, and Department of Pharmaceutical Sciences, University of California, Irvine. 949-824-4486. sctsai@uci.edu

John Crosby. School of Chemistry, University of Bristol, United Kingdom. +44 (0) 117 928 8445. John.Crosby@bristol.ac.uk

Matthew P. Crump. School of Chemistry, University of Bristol, United Kingdom. +44 (0) 117 331 7163. matt.crump@bristol.ac.uk

Table of Contents

Table S1. DpsC crystallographic data collection and refinement statistics.

Figure S1. DpsC self-acylation with different acyl-CoA substrates.

Figure S2. *In vitro* kinetic assay of DpsC self-acylation.

Figure S3. *In vitro* assays for DpsC acyl-transfer to DpsG.

Figure S4. The differences in spatial orientation between the DpsC and *EcFabH* active site residues.

Figure S5. SA omit maps of the DpsC active site.

Figure S6. Comparison of the DpsC active site with the *EcFabH* active site focusing on Leu93 (DpsC) and Phe87 (*EcFabH*).

Figure S7. Synthesis of the phosphorylated PPant analogue **4**.

Figure S8. Sequence alignment of putative DpsC homologues.

Figure S9. ^1H NMR assignment of **2**

Figure S10. ^{13}C NMR spectrum of **2**

Figure S11. ^1H NMR assignment of **3**

Figure S12. ^{13}C NMR spectrum of **3**

	<i>apo</i> -DpsC	acetyl-DpsC	propionyl-DpsC	butyryl-DpsC	DpsC co-crystal with 4
PDB ID:	5TT4	4XS7	4XSA	4XSB	4XS9
Crystallization	0.18 M sodium citrate, 26 % PEG 3350	0.18 M sodium citrate, 26 % PEG 3350	0.18 M sodium citrate, 26 % PEG 3350	0.18 M sodium citrate, 26 % PEG 3350	0.18 M sodium citrate, 26 % PEG 3350
Crystallographic Data					
Wavelength (Å)	0.9999	0.9775	1.0000	0.9999	0.9795
Space Group	P6 ₅ 22	P6 ₅ 22	P6 ₅ 22	P6 ₅ 22	P6 ₅ 22
Cell Dimension a, b, c (Å)	90.033, 90.033, 304.689	91.213, 91.213, 315.643	91.477, 91.477, 316.833	91.382, 91.382, 315.783	89.702, 89.702, 302.704
	$\alpha=\beta=90^\circ$, $\gamma=120^\circ$	$\alpha=\beta=90^\circ$, $\gamma=120^\circ$	$\alpha=\beta=90^\circ$, $\gamma=120^\circ$	$\alpha=\beta=90^\circ$, $\gamma=120^\circ$	$\alpha=\beta=90^\circ$, $\gamma=120^\circ$
Resolution (Å)	50.00 - 2.50	50.00-2.40	50.00 - 2.40	50.00 - 2.20	50.00-2.30
No. of observations	557086	500940	857439	411366	479239
No. of unique observations	26403	31516	40753	40709	33191
Completeness %	99.3 (98.8)	100.00 (100.00)	99.6 (99.2)	99.9 (100)	100.0 (100.0)
I/ σ (I)	24.1 (6.0)	18.6 (4.3)	25.0 (5.3)	18.4 (2.6)	19.8 (6.0)
R _{merge} %	14.2 (65.0)	13.9 (79.9)	16.5 (75.9)	11.3 (81.9)	17.8 (44.3)
Redundancy	21.1	15.9	22.5	10.1	14.4
Refinement					
Resolution (Å)	50.00 - 2.50 (2.59 - 2.50)	50.00 - 2.40 (2.49 - 2.40)	50.00 - 2.4 (2.49 - 2.40)	50.00 - 2.20 (2.28 - 2.20)	50.00 - 2.30 (2.38 - 2.30)
No. of protein atoms	5058	5068	5102	5104	5073
No. of ligand atoms	0	0	0	0	52
No. of water atoms	173	248	572	431	316
R _{free} %	20.88 (23.47)	21.57 (29.88)	20.29 (24.10)	22.49 (31.98)	19.76 (23.02)
R _{crys} %	16.18 (18.96)	17.70 (20.80)	16.64 (18.10)	17.79 (25.03)	15.93 (17.81)
Geometry					
RMS bonds (Å)	0.008	0.023	0.009	0.008	0.008
RMS angles (°)	1.09	1.40	1.17	1.16	1.10
Ramachandran Favored (%)	98.00	96.00	97.00	96.00	98.00
Ramachandran Allowed (%)	1.55	3.55	2.56	3.41	1.70
Ramachandran Disallowed (%)	0.45	0.45	0.44	0.59	0.30
Average B-factors (Å²)					
Protein	32.40	34.30	17.50	29.90	29.00
Water	33.80	35.30	26.40	35.70	40.20
Ligands	N/A	N/A	N/A	N/A	33.10

Table S1. DpsC crystallographic data collection and refinement statistics.

*Numbers in parentheses denote the highest resolution shell.

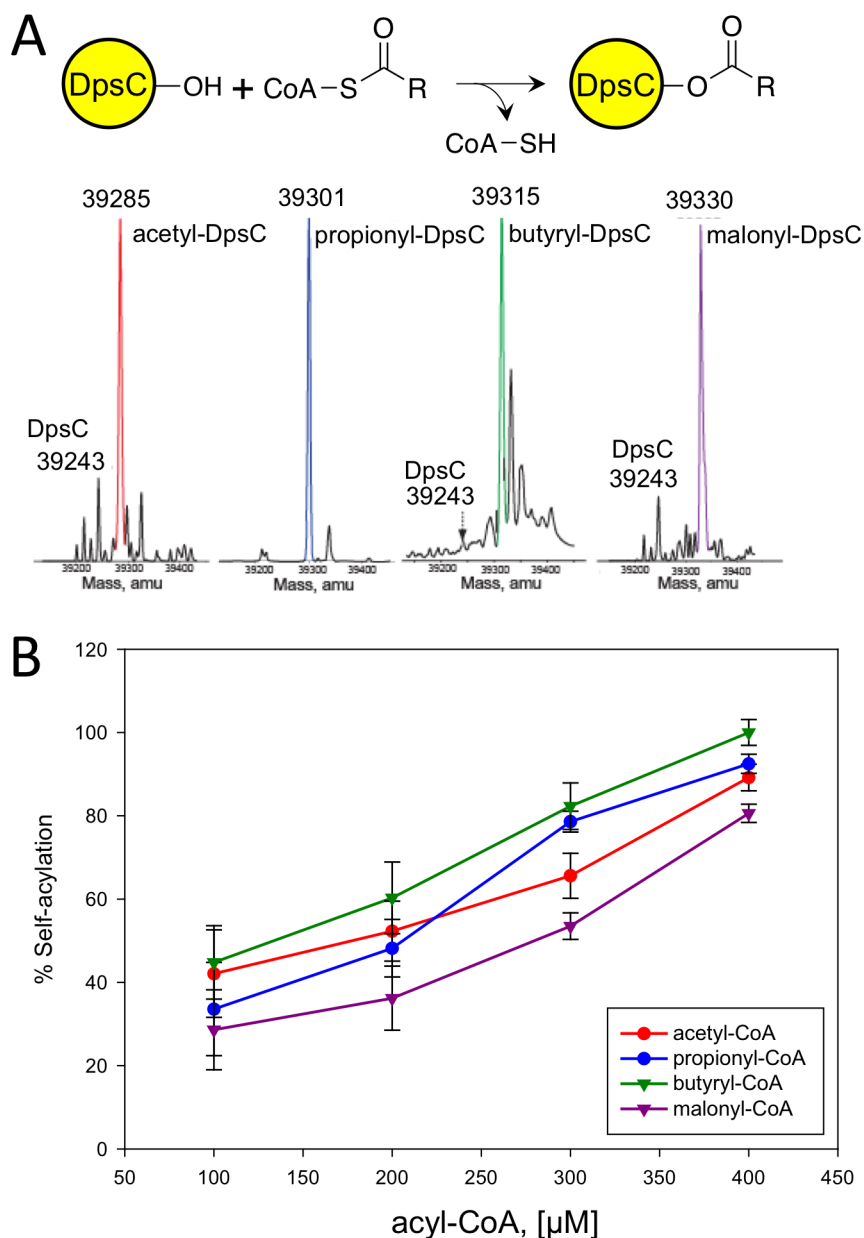
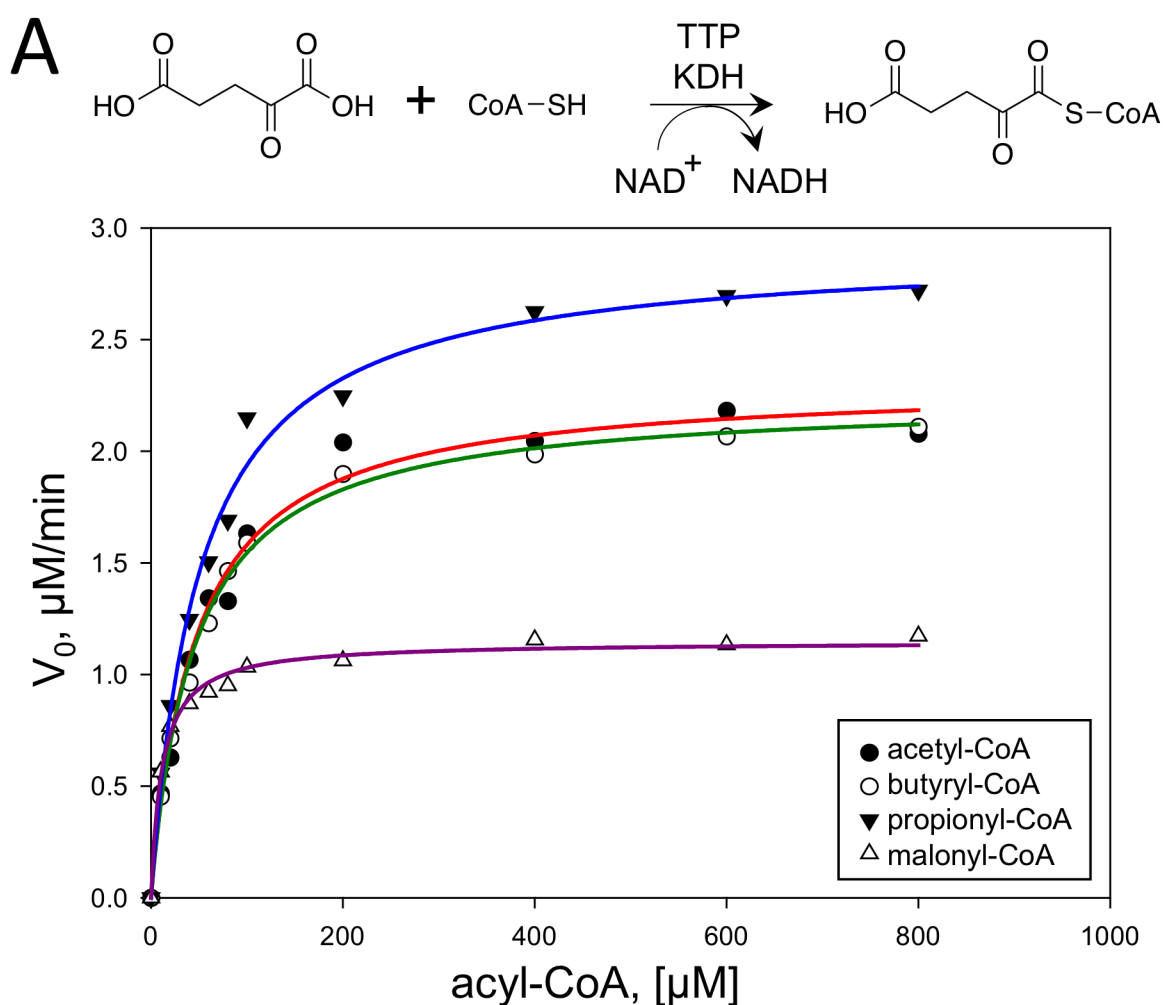


Figure S1. DpsC self-acylation with different acyl-CoA substrates. (A) Deconvolved ESI-MS spectra of purified DpsC after incubation with different CoA derivatives (acetyl-CoA, propionyl-CoA, butyryl-CoA and malonyl-CoA). ESI-MS analysis indicated that DpsC does not selectively load propionate. Calculated masses of DpsC, acetyl-DpsC, propionyl-DpsC, butyryl-DpsC and malonyl-DpsC are 39248, 39287, 39304, 39315 and 39334 Da respectively. (B) Graph showing the self-acylation efficiency of DpsC towards different starter units in non-saturating conditions. Higher affinity for propionate was not observed.



B

Kinetic parameter	acetyl-CoA	propionyl-CoA	butyryl-CoA	malonyl-CoA
V_{\max} (μM.min ⁻¹)	2.31 ± 0.06	2.91 ± 0.07	2.24 ± 0.03	1.15 ± 0.04
K_M (μM)	46.14 ± 4.81	50.21 ± 4.35	44.96 ± 2.72	11.35 ± 2.21
k_{cat} (min ⁻¹)	0.12	0.14	0.11	0.06
k_{cat}/K_M (μM ⁻¹ .min ⁻¹)	2.6x10 ⁻³ ± 3x10 ⁻⁴	2.8x10 ⁻³ ± 2x10 ⁻⁴	2.6x10 ⁻³ ± 2x10 ⁻⁴	5.3x10 ⁻³ ± 1x10 ⁻³

Figure S2. *In vitro* kinetic assay of DpsC self-acylation. (A) Schematic representation of the mechanism of KDH assay and Michaelis-Menten plots for the self-acylation of DpsC. (B) Kinetic parameters were calculated by fitting the Michaelis-Menten curve to the experimental data.

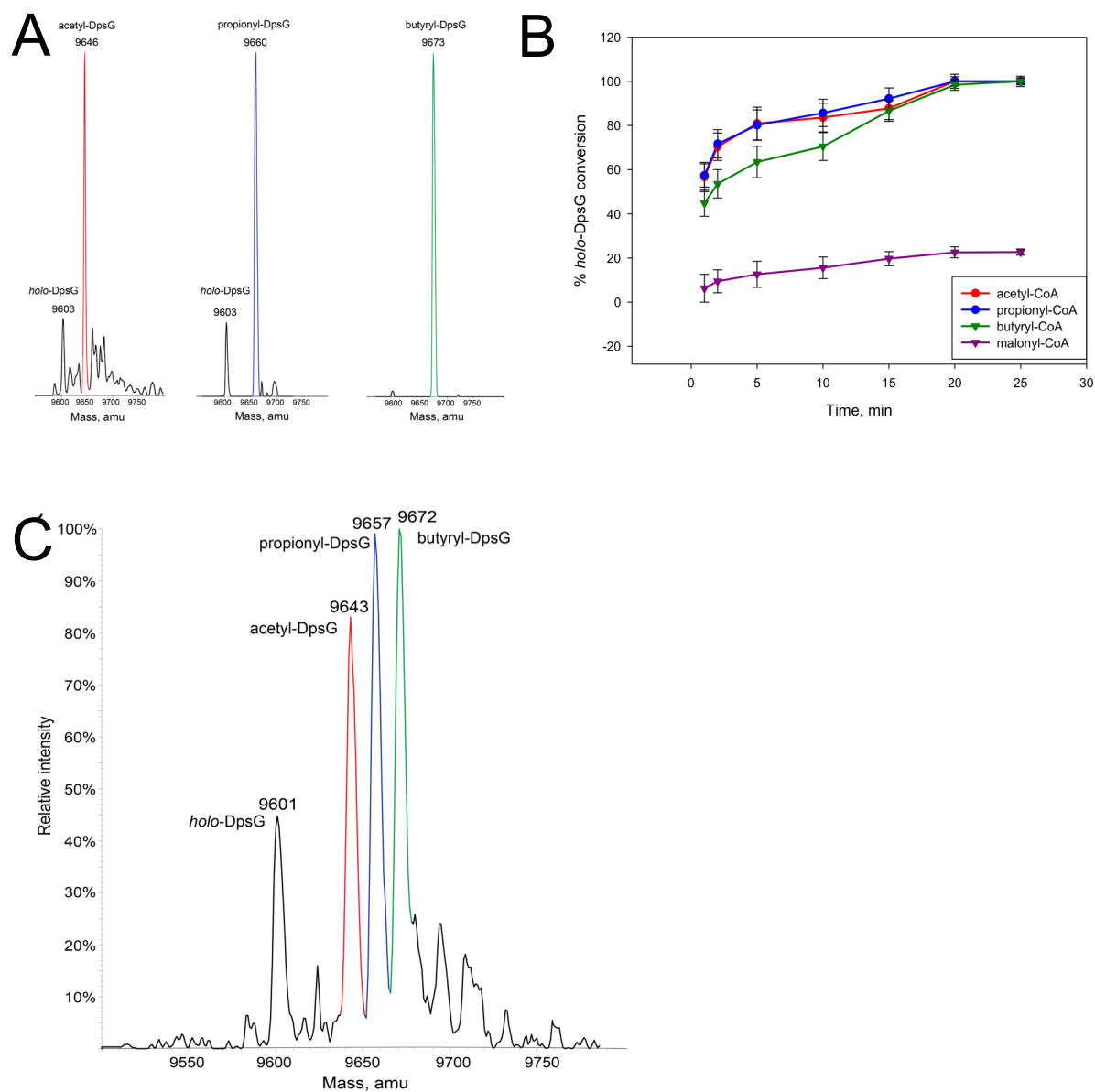


Figure S3. *In vitro* assays for DpsC acyl-transfer to DpsG. (A) Deconvolved ESI-MS spectrum showing acyltransferase activity of DpsC when incubated with *holo*-DpsG and CoA derivatives. Calculated masses for *holo*-, acetyl-, propionyl- and butyryl-DpsG are 9604, 9646, 9660 and 9674 Da respectively. (B) The rate of conversion of *holo*-DpsG to the acylated form for all starter units. (C) Deconvolved ESI-MS spectrum of *holo*-DpsG components from acyltransferase activity by DpsC. No selective transfer of propionate onto DpsG was observed when the enzymes were incubated in a pool of different starter units.

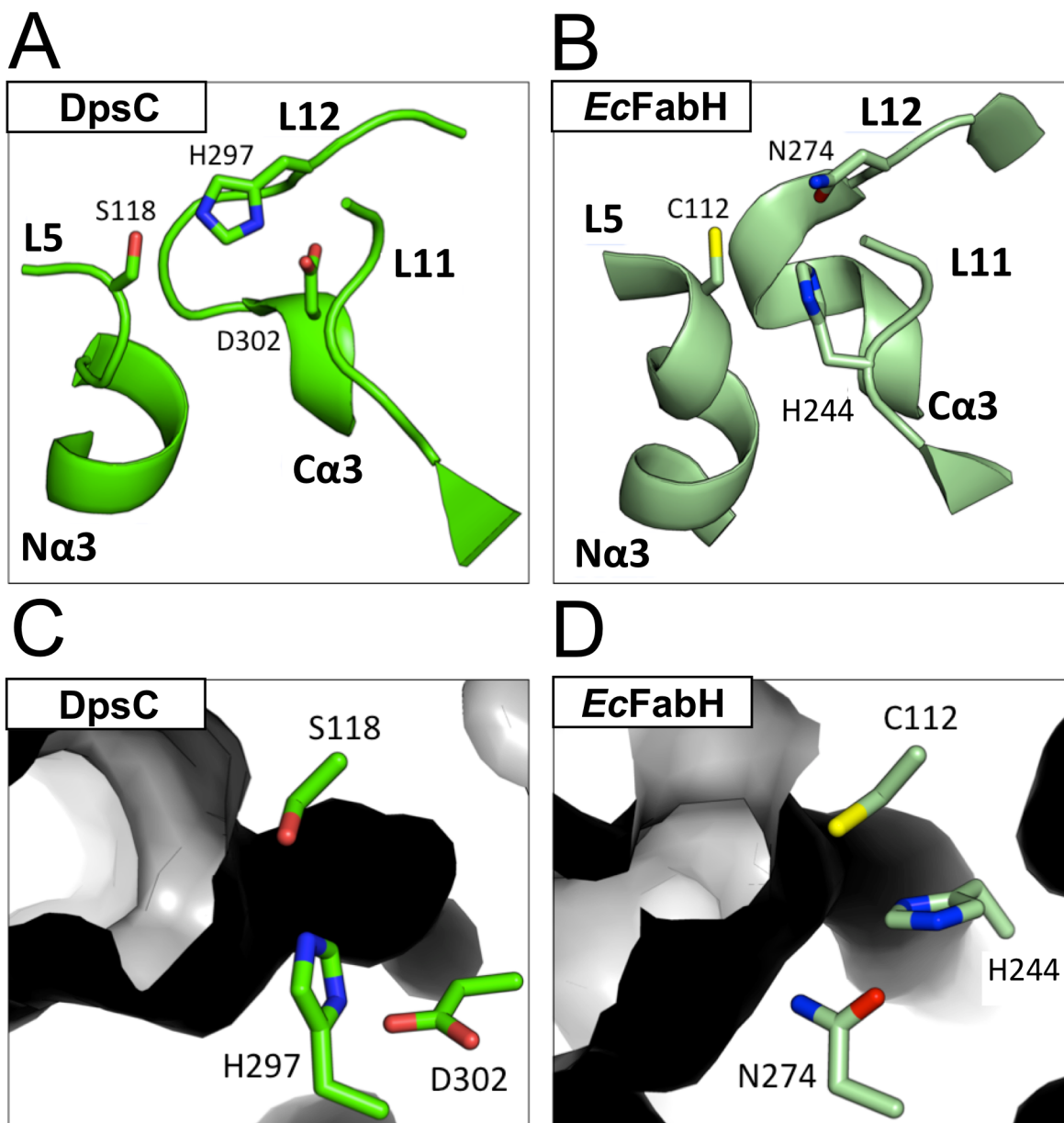


Figure S4. The differences in spatial orientation between the DpsC and *EcFabH* active site residues. (A) In DpsC, Ser118, His297, and Asp302, are located on L5, L12, and Ca3, respectively. (B) In *EcFabH*, Cys112, His244, and Asn274, are located on L5, L12, and L11, respectively. (C) His297 and Asp302 of DpsC are behind the active site pocket and His297 is positioned so that the aromatic ring stacks against the side of the pocket. (D) His244 and Asn274 of *EcFabH* are positioned to the side of the active site pocket with both of their side chains able to form hydrogen bonds with substrates in the active site.

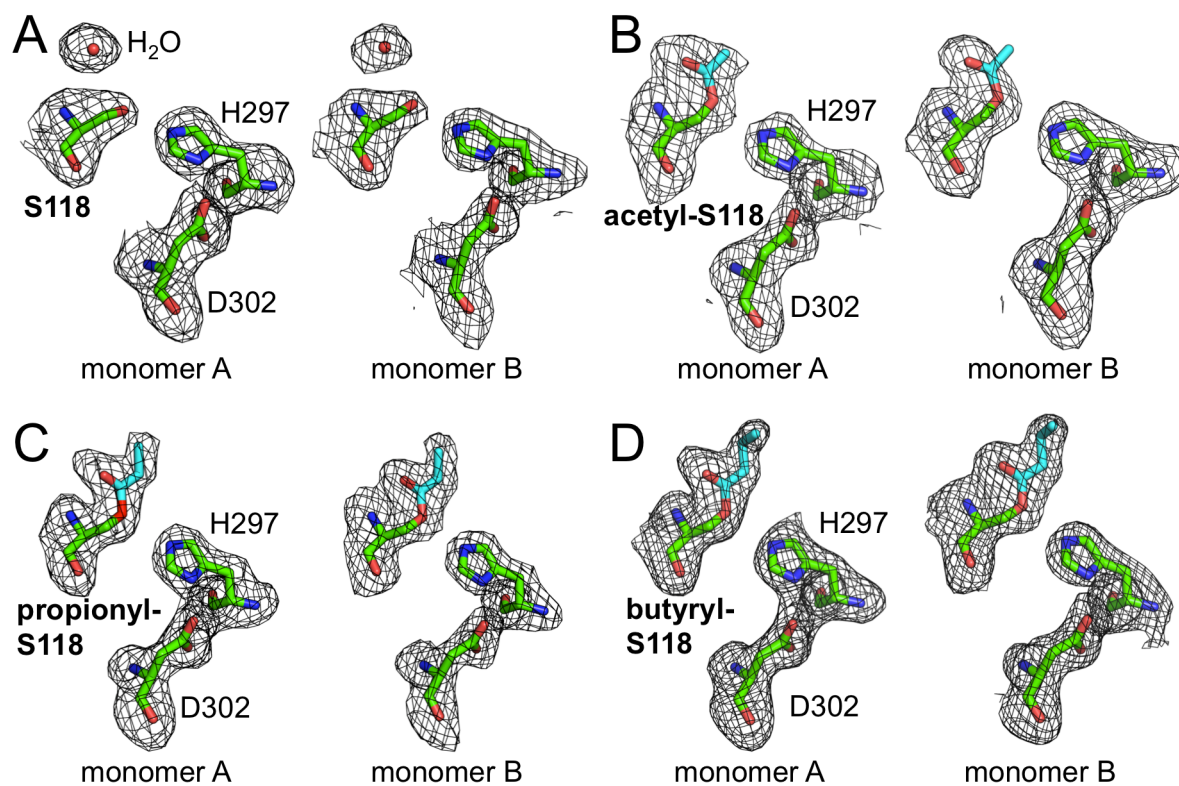


Figure S5. SA omit maps of the DpsC active site. The active site of monomer A is on the left (residues labeled) and the active site of monomer B is on the right (residues unlabeled). Acyl groups are colored in cyan. (A) Apo-DpsC. (B) Acetyl-DpsC. (C) Propionyl-DpsC. (D) Butyryl-DpsC.

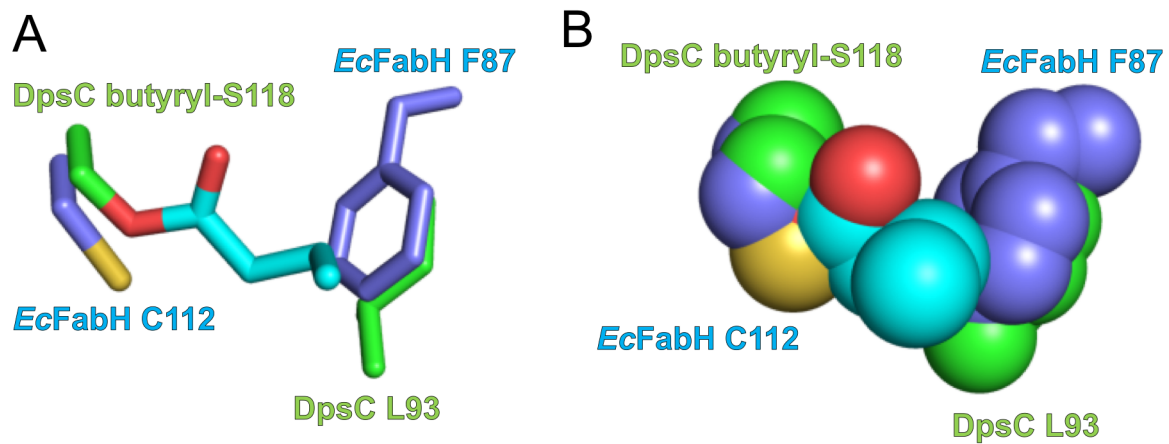


Figure S6. Comparison of the DpsC active site with the *EcFabH* active site focusing on Leu93 (DpsC) and Phe87 (*EcFabH*).

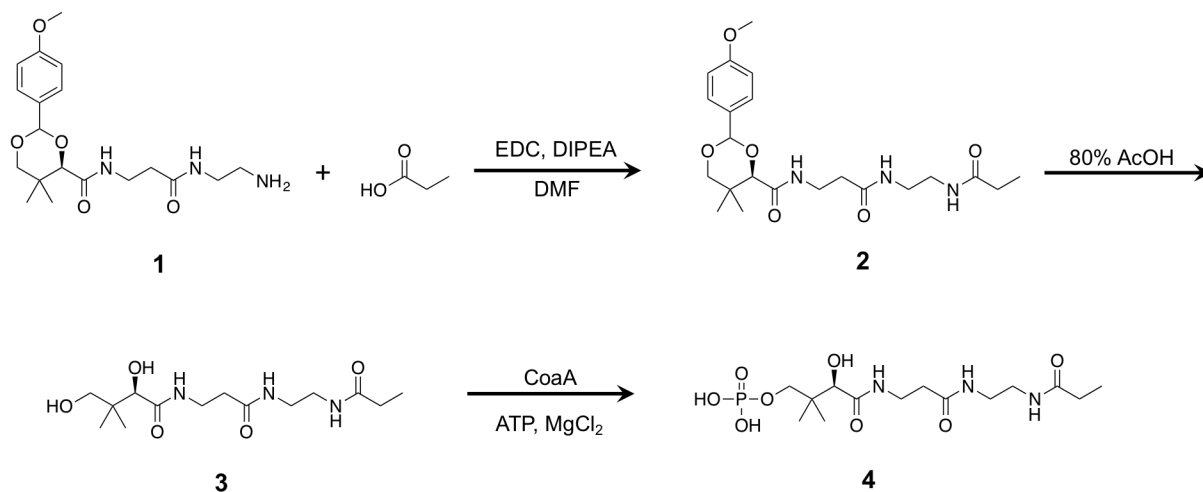


Figure S7. Synthesis of the phosphorylated PPant analogue **4**. Protected pantetheine amine **1** can be coupled with a propanoic acid, and deprotection yields the pantetheine analogue **3** with an amide linkage. **3** can be directly phosphorylated using the CoaA kinase to form a substrate mimic **4** for co-crystallization.

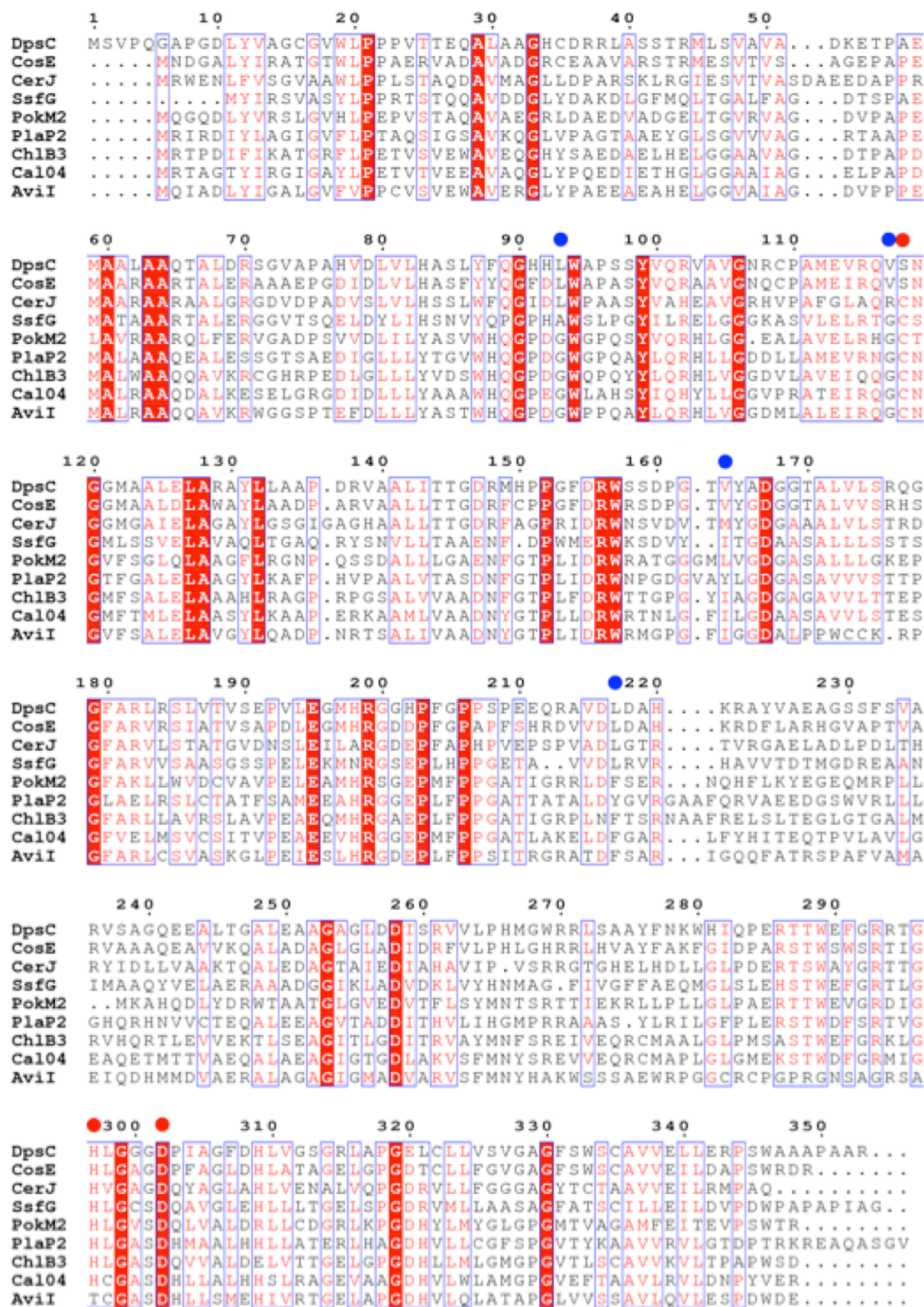


Figure S8. Sequence alignment of putative DpsC homologues. The active site residues are marked with a red dot and residues in the acyl binding region are marked with a blue dot.

Figure S9. ¹H NMR assignment of compound 2

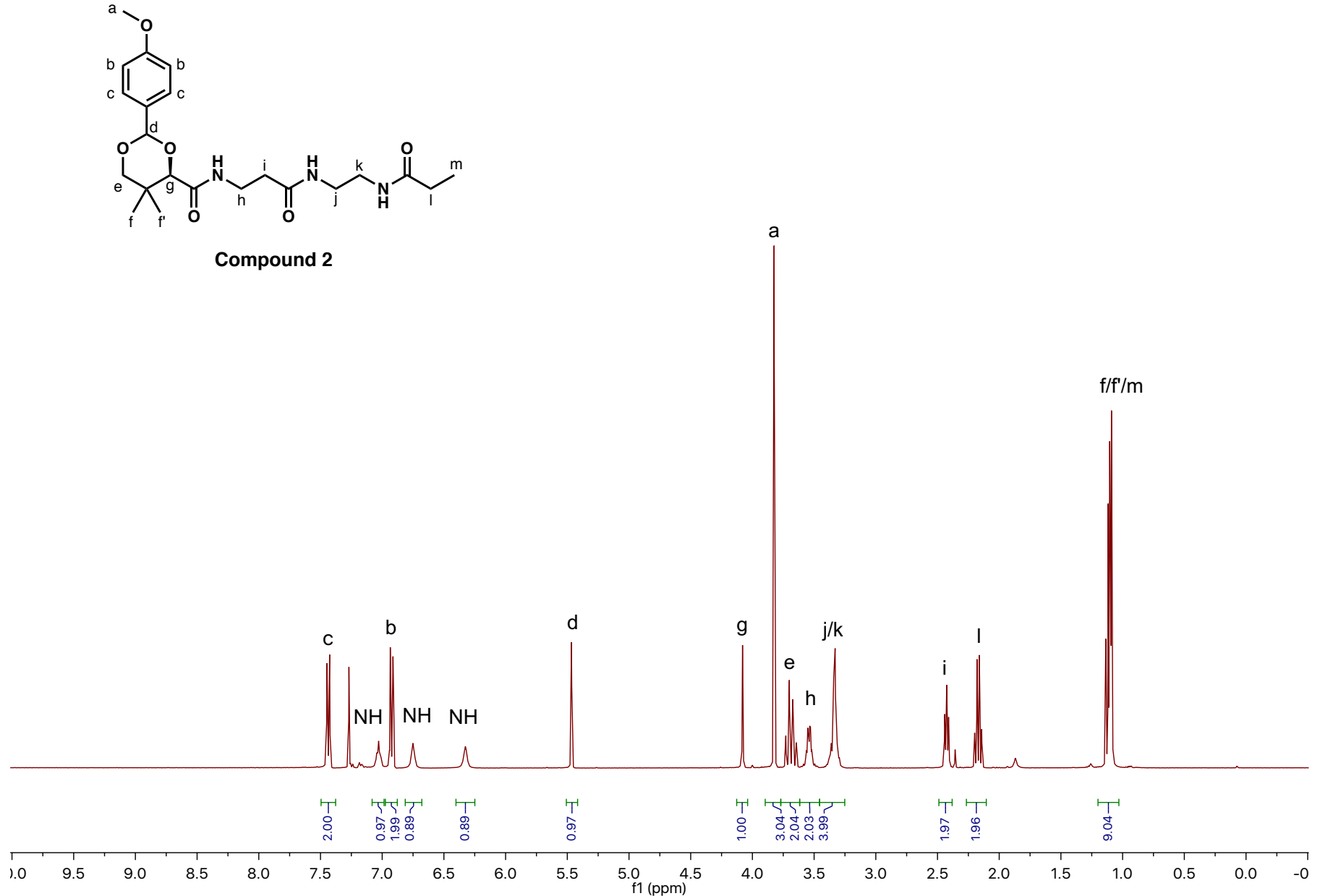
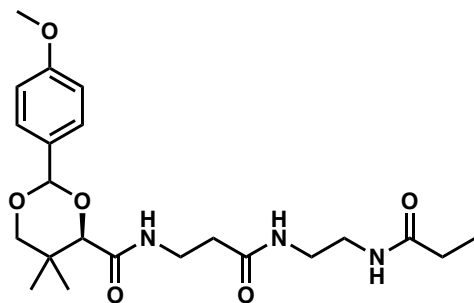


Figure S10. ¹³C NMR spectrum of compound 2



Compound 2

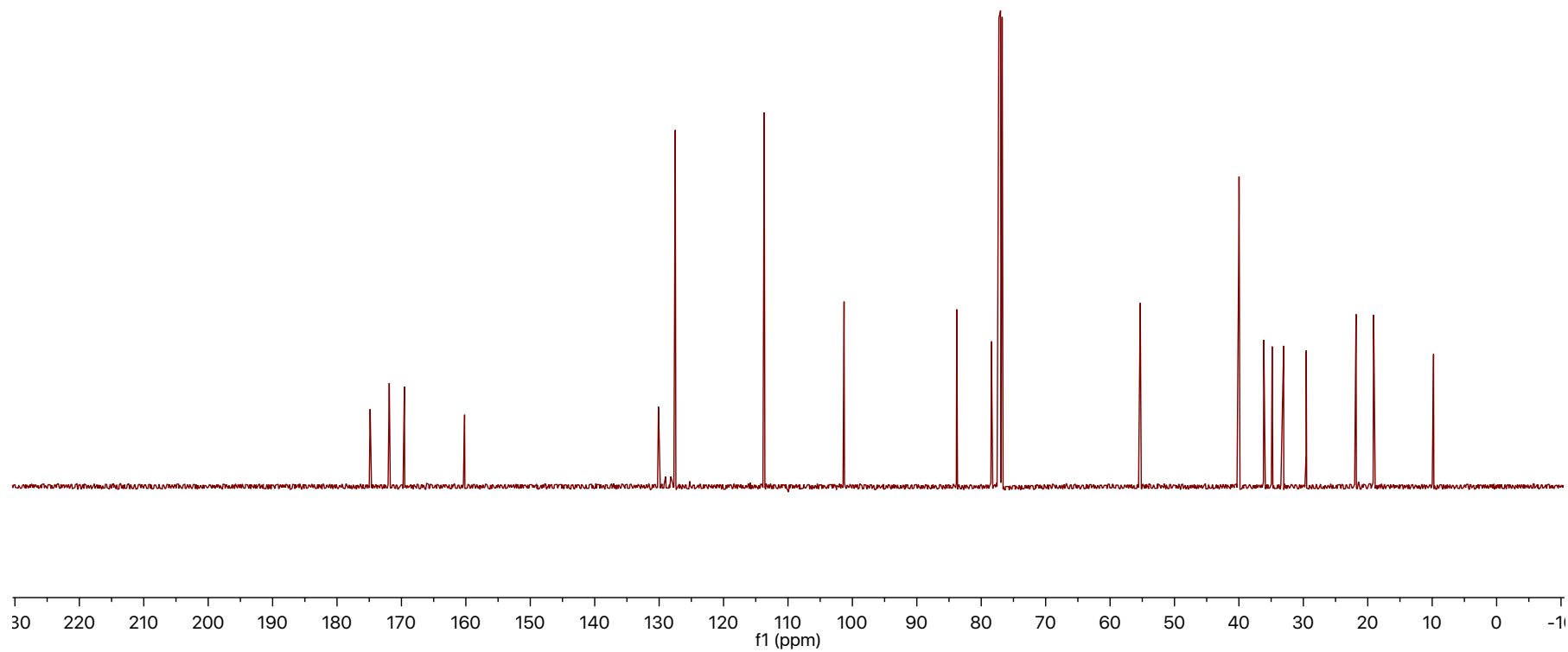
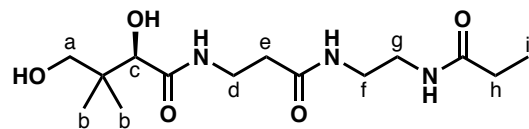


Figure S11. ¹H NMR assignment of compound 3



Compound 3

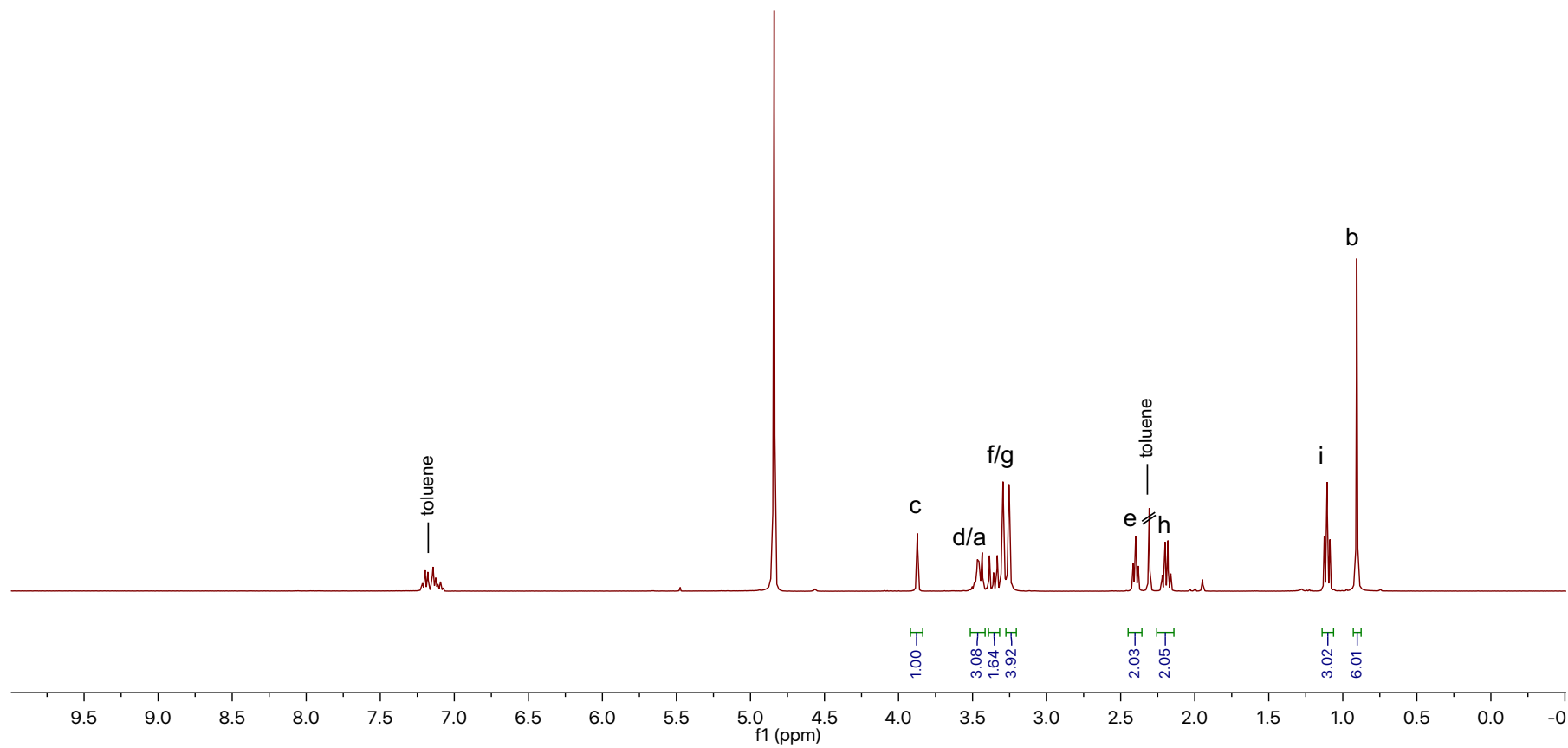
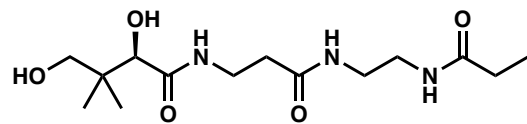


Figure S12. ¹³C NMR spectrum of compound 3



Compound 3

